Early−Late Heterotetranuclear Complexes ($TiRh_3$) with Bridging Sulfido Ligands: Ligand Replacement Reactions and Catalytic Activity in Hydroformylation of Olefins

Miguel A. Casado, Jesús J. Pérez-Torrente, Miguel A. Ciriano,* and Luis A. Oro*

Departamento de Química Inorgánica, Instituto de Ciencia de Materiales de Aragón, Universidad de Zaragoza-CSIC, 50009 Zaragoza, Spain

Arantxa Orejón and Carmen Claver*

Departament de Química Física i Inorgànica, Facultat de Química, Universitat Rovira i Virgili, Plaça Imperial Tàrraco 1, 43005 Tarragona, Spain

Received March 4, 1999

The tetranuclear early−late heterobimetallic ($TiRh_3$) complexes $[CpTi(\mu_3\text{-}S)_3\{Rh(diolef)\}_3]$ (diolef = tfbb (**1**), cod (**2**)) in the presence of P-donor ligands are active precursors in the hydroformylation of hex-1-ene and styrene under mild conditions of pressure and temperature. A 96% conversion to aldehydes and 77% regioselectivity for the linear aldehyde is obtained in the hydroformylation of hex-1-ene using PPh_3 (P/Rh = 2−4) as the P-donor ligand at 5 bar and 353 K. Hydroformylation of styrene under similar conditions (10 bar) gives 70% conversion and 88% regioselectivity in favor of 2-phenylpropanal. The reaction of $[CpTi(\mu_3\text{-}S)_3\{Rh(CO)_2\}_3]$ (**3**) with monodentate P-donor ligands results in the selective synthesis of the C_3 isomer of the complexes $[CpTi(\mu_3\text{-}S)_3Rh_3(CO)_3(PR_3)_3]$. The compound $[CpTi(\mu_3\text{-}S)_3Rh_3(CO)_3(PPh_3)_3]$ (**5**) reacts reversibly with carbon monoxide to give the 62-electron valence clusters $[CpTi(\mu_3\text{-}S)_3Rh_3(\mu\text{-}CO)(CO)_4(PPh_3)_2]$ (**4b**) and $[CpTi(\mu_3\text{-}S)_3Rh_3(\mu\text{-}CO)(CO)_3(PPh_3)_3]$ (**4c**), which are in equilibrium. High-pressure NMR spectroscopic studies have shown that both clusters are also formed under hydroformylation conditions. A multinuclear NMR spectroscopic investigation of the replacement reactions shows that $[CpTi(\mu_3\text{-}S)_3Rh_3(CO)_5(PPh_3)]$ (**4a**), **4b**, and **4c** are intermediary species in the replacement reactions leading to **5**, the decarbonylation of **4c** being the key step for the observed stereoselectivity. The reaction of **3** with diphosphines gives the complexes $[CpTi(\mu_3\text{-}S)_3Rh_3(\mu\text{-}P{-}P)(CO)_4]$ (P−P = 1,2-bis(diphenylphosphine)ethane (dppe); 1,3-bis(diphenylphosphine)propane, (dppp)), $[CpTi(\mu_3\text{-}S)_3Rh_3(CO)_4(\eta^2\text{-}(R)\text{-BINAP})]$, and $[CpTi(\mu_3\text{-}S)_3Rh_3(\mu\text{-dppe})(CO)_2(\eta^2\text{-dppe})]$, in which the heterotetranuclear metal framework is maintained.

Introduction

Bi- and polymetallic complexes should be capable of providing novel catalytic chemistry which is unavailable with mononuclear homogeneous catalysts. However, fragmentation has been a major and continuing problem in these catalyst systems.[1−3]

With respect to hydroformylation catalysis, several papers have been published dealing also with bimetallic cooperativity.[4−7] During the past decade, dinuclear rhodium thiolate complexes have been the subject of much interest. Thus, for $[Rh_2(\mu\text{-}SR)_2(CO)_2(PR_3)_2]$ a catalytic cycle, based on spectroscopic observations and theoretical calculations, in which the dinuclear framework is retained for all steps is proposed.[4] However, an investigation of catalyst crossover reactions suggests the presence of mononuclear species.[5] On the other hand, early−late Zr−Rh and Ti−Rh heterobimetallic systems have been shown to be efficient hydroformylation catalysts.[6] In these systems, considering the tetrahedral geometry around the zirconium atom, both rhodium atoms are maintained in proximity to each other and a cooperative effect has been suggested.

An important step forward in the search for catalytically active polynuclear metal complexes has been made

(1) *Catalysis by Di- and Polynuclear Metal Cluster Complexes*; Adams, R. D., Cotton, F. A., Eds.; Wiley-VCH: New York, 1998.

(2) Chaloner, P. A.; Esteruelas, M. A.; Joó, F.; Oro, L. A. In *Homogeneous Hydrogenation;* Kluwer Academic: Dordrecht, The Netherlands, 1994.

(3) Gao, H.; Angelici, R. J. *Organometallics* **1998**, *17*, 3063.

(4) (a) Kalck, Ph. In *Organometallics in Organic Syntheses;* De Meijere, A., tom Dieck, H., Eds.; Springer-Verlag: Berlin, 1987; pp 297−320. (b) Kalck, Ph. *Pure Appl. Chem.* **1989**, *61*, 967. (c) Kalck, Ph.; Peres, Y.; Queau, R.; Molinier, J.; Escaffre, P.; Oliveira, E. L.; Peyrille, B. *J. Organomet. Chem.* **1992**, *426*, C16.

(5) Davis, R.; Epton, J. W.; Southern, T. G. *J. Mol. Catal.* **1992**, *77*, 159.

(6) (a) Choukroun, R.; Dahan, F.; Gervais; D.; Rifaï, Ch. *Organometallics* **1990**, *9*, 1982. (b) Senocq, F.; Randrialimanana, C.; Thorez, A.; Kalck, Ph.; Choukroun, R.; Gervais, D. *J. Mol. Catal.* **1986**, *35*, 213. (c) Trzeciak, A. M.; Ziólkowski, K. J.; Choukroun, R. *J. Mol. Catal.* **1996**, *110*, 135.

(7) (a) Broussard, M. E.; Juma, B.; Train, S. G.; Peng, W.-J.; Laneman, S. A.; Stanley, G. G. *Science* **1993**, *260*, 1784. (b) Süss-Fink, G. *Angew. Chem., Int. Ed. Engl.* **1994**, *33*, 67.

10.1021/om990155j CCC: $18.00
Publication on Web 07/10/1999

by Stanley et al.[7] The bimetallic complex $[Rh_2(nbd)_2(et,ph\text{-}P4)](BF_4)_2$ (et,ph-P4 = $(Et_2PCH_2CH_2)(Ph)PCH_2P(Ph)(CH_2CH_2PEt_2)$) is an excellent hydroformylation catalyst for olefins, combining high activity with high regioselectivity. A mechanism involving bimetallic cooperativity between the two rhodium centers in the form of an intramolecular hydride transfer is proposed.

The importance of heterometallic complexes for homogeneous catalysis and supported molecular catalysis is based on the reasonable expectation that two or more adjacent metal centers may offer possibilities for cooperative reactivity and synergism. Thus, in recent years, numerous examples of cluster catalysis with heterometallic complexes have appeared in the literature.[8] We have previously reported that some heterodinuclear Ru−Ir or Ru−Rh complexes are more active catalysts for the reduction of olefins than are the mononuclear parent compounds. According to detailed kinetic studies, the dinuclear framework is maintained during the catalysis but the hydrogenation proceeds mainly at one metal center, the other metal acting as the core of a metallo ligand of variable electronic density.[9] On the other hand, and to the best of our knowledge, no homogeneous heterotetranuclear catalytic systems containing titanium and rhodium have so far been reported.

We have recently prepared an unusual family of early−late complexes of general formula $[CpTi(\mu_3\text{-}S)_3\{Rh(L_2)\}_3]$ (L_2 = diolefin, L = CO)[10] which exhibit an outstanding stability of the heterotetranuclear framework and therefore would be good candidates for polymetallic hydroformylation catalysis. We report in this paper the hydroformylation of olefins using $[CpTi(\mu_3\text{-}S)_3\{Rh(cod)\}_3]$ and $[CpTi(\mu_3\text{-}S)_3\{Rh(tfbb)\}_3]$ as catalyst precursor complexes. The synthesis and characterization of early−late heterotetranuclear complexes containing P-donor ligands, which are relevant to the hydroformylation experiments, are also described. In addition, the investigation of the selectivity of the substitution reactions by monodentate P-donor ligands in the carbonyl complex $[CpTi(\mu_3\text{-}S)_3\{Rh(CO)_2\}_3]$ and high-pressure NMR (HPNMR) spectroscopy have provided valuable information for the elucidation of the structure of the precursors in solution under hydroformylation conditions.

Results

Replacement Reactions on $[CpTi(\mu_3\text{-}S)_3\{Rh(CO)_2\}_3]$ by P-Donor Ligands. The heterotetranuclear complex $[CpTi(\mu_3\text{-}S)_3\{Rh(CO)_2\}_3]$ (**3**), obtained by carbonylation of the diolefinic complexes $[CpTi(\mu_3\text{-}S)_3\{Rh(diolefin)\}_3]$ (diolefin = tfbb (tetrafluorobenzobarrelene) (**1**), cod (1,5-cyclooctadiene) (**2**)) at atmospheric pressure, reacts with triphenylphosphine to give selectively a single isomer of the tricarbonyl heterotetranuclear complex $[CpTi(\mu_3\text{-}S)_3\{Rh(CO)(PPh_3)\}_3]$ (**5**) as result of monosubstitution at each rhodium center.[10b] The selectivity observed for the reaction of **3** with triphenylphosphine is general, since more basic or more sterically demanding trialkylphosphines also give a single isomer. Thus, the reaction of **3** with 3 molar equiv of PMe_3 or PCy_3 gives the trisubstituted complexes $[CpTi(\mu_3\text{-}S)_3\{Rh(CO)(PMe_3)\}_3]$ (**6**) and $[CpTi(\mu_3\text{-}S)_3\{Rh(CO)(PCy_3)\}_3]$ (**7**), respectively, which are isolated as yellow microcrystalline solids. Both complexes exhibit the molecular ions in the mass spectra and show strong ν(CO) absorptions in the IR spectra shifted to lower frequencies relative to $[CpTi(\mu_3\text{-}S)_3\{Rh(CO)(PPh_3)\}_3]$ (**5**), as is to be expected for the coordination of more basic ligands to the rhodium atoms. Interestingly, the $^{31}P\{^1H\}$ NMR spectra of both complexes show a doublet indicating the equivalence of the phosphine ligands and therefore the exclusive formation of the C_3 isomer.

In the same way, complex **3** reacts with 3 equiv of the phosphite ligands $P(OPh)_3$, $P(OMe)_3$, or $P(o\text{-}OC_6H_4{}^tBu)_3$ to give the complexes $[CpTi(\mu_3\text{-}S)_3\{Rh(CO)(P(OR)_3)\}_3]$ (R = Ph (**8**), Me (**9**), $C_6H_4{}^tBu$ (**10**)) as yellow microcrystalline solids in good yield. Monosubstitution at the rhodium centers is confirmed by the IR spectra, and once again, the $^{31}P\{^1H\}$ NMR spectra of the complexes corroborate the selective synthesis of the C_3 isomer. The possible isomers for the complexes $[CpTi(\mu_3\text{-}S)_3\{Rh(CO)(PR_3)\}_3]$ (**5**−**11**), assuming a free rotation of the Cp ring for the symmetry assignment, are shown in Chart 1.

Chart 1

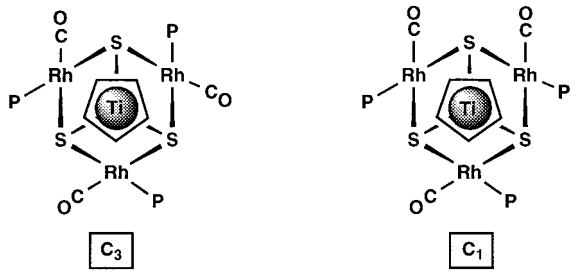

Interestingly, the one-pot synthesis of the complexes **5**−**10** is possible from the diolefinic complexes $[CpTi(\mu_3\text{-}S)_3\{Rh(diolef)\}_3]$. Thus, the sequential reaction of complex **1** or **2** with carbon monoxide followed by 3 molar equiv of the corresponding phosphine or phosphite ligand leads to the complex $[CpTi(\mu_3\text{-}S)_3\{Rh(CO)(PR_3)\}_3]$.

The related compound with the water-soluble monosulfonated triphenylphosphine (TPPMS) ligand $[CpTi(\mu_3\text{-}S)_3\{Rh(CO)(TPPMS)\}_3]$ (**11**) can be formed by reaction of **3** with TPPMS, although it is always isolated impure in low yield. However, the exchange of the triphenylphosphine ligands in $[CpTi(\mu_3\text{-}S)_3\{Rh(CO)(PPh_3)\}_3]$ (**5**) with TPPMS in THF provides a more convenient route to **11**, overcoming side reactions.[11] Complex **11** is an orange solid which is obtained as the monohydrate in good yield. The $^{31}P\{^1H\}$ NMR spectrum in CD_3OD shows a doublet, and a strong ν(CO) absorption is observed in the IR spectrum, as expected for the C_3 isomer.

(8) (a) Braunstein, P.; Rosé, J. In *Comprehensive Organometallic Chemistry II*; Stone, F. G. A., Abel, E., Adams, R. D., Eds.; Pergamon: London, 1995. (b) Braunstein, P.; Rosé, J. In *Metal Clusters in Chemistry*; Braunstein, P., Oro, L. A., Raithby, P. R., Eds.; Wiley-VCH: Weinheim, Germany, in press.

(9) (a) Esteruelas, M. A.; García, M. P.; López, A. M.; Oro, L. A. *Organometallics* **1991**, *10*, 127. (b) Esteruelas, M. A.; García, M. P.; López, A. M.; Oro, L. A. *Organometallics* **1992**, *11*, 702.

(10) (a) Casado, M. A.; Ciriano, M. A.; Edwards, A. J.; Lahoz, F. J.; Oro, L. A.; Pérez-Torrente, J. J. *Organometallics* **1999**, *18*, 3025. (b) Atencio, R.; Casado, M. A.; Ciriano, M. A.; Lahoz, F. J.; Pérez-Torrente, J. J.; Tiripicchio, A.; Oro, L. A. *J. Organomet. Chem.* **1996**, *514*, 103.

(11) (a) Joó, F.; Kovács, J.; Kathó, A.; Bényei, A. C.; Decuir, T.; Darensbourg, D. J. *Inorg. Synth.* **1998**, *32*, 1. (b) Joó, F.; Kathó, A. *J. Mol. Catal. A.* **1997**, *116*, 3.

Chart 2

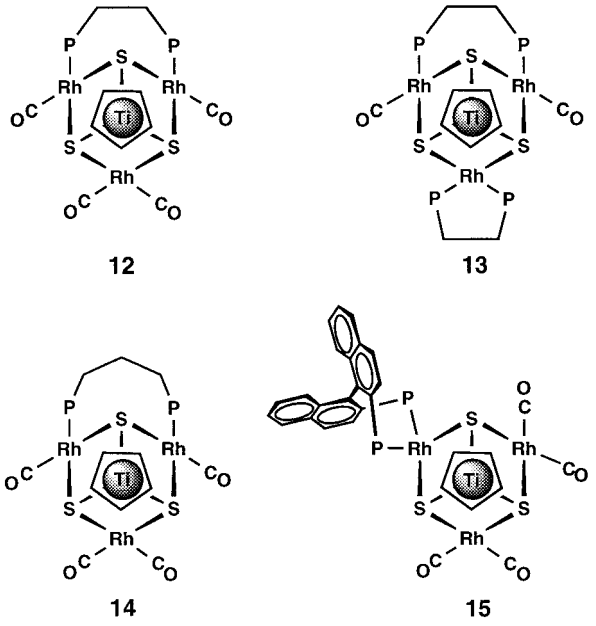

Chart 3

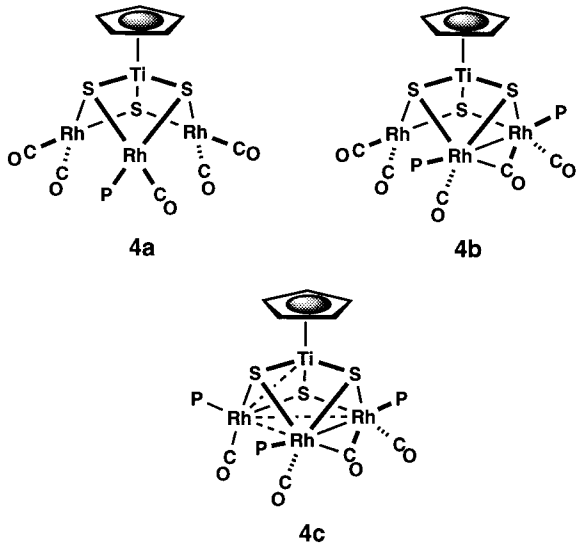

The substitution reactions on $[CpTi(\mu_3\text{-}S)_3\{Rh(CO)_2\}_3]$ (**3**) with diphosphines are strongly dependent on the nature of the diphosphine. Usually, only 1 molar equiv of diphosphine is easily incorporated into the heterotetranuclear framework (dppp or BINAP); nevertheless, in some cases, the replacement of four of the carbonyl ligands allows the introduction of 2 molar equiv of diphosphine (dppe).

The reaction of **3** with 1 molar equiv of dppe gives the complex $[CpTi(\mu_3\text{-}S)_3Rh_3(CO)_4(\mu\text{-dppe})]$ (**12**), while reaction with 2 molar equiv of diphosphine gives $[CpTi(\mu_3\text{-}S)_3Rh_3(\mu\text{-dppe})(CO)_2(\eta^2\text{-dppe})]$ (**13**). Both complexes are obtained as orange solids in good yield and have been fully characterized by elemental analysis and mass and NMR spectroscopy. In particular, the $^{31}P\{^1H\}$ NMR spectra allow us to propose the C_s structures shown in Chart 2. Complex **12** displays a doublet centered at 30.7 ppm ($J_{Rh-P} = 163$ Hz) in the $^{31}P\{^1H\}$ NMR, as expected for a bridging coordination mode of the dppe ligand[12] having equivalent phosphorus atoms. The $^{31}P\{^1H\}$ NMR spectrum of complex **13** displays two doublets, indicating the chemical equivalence of both phosphorus atoms for each diphosphine. The presence of a high-field doublet centered at 65.5 ppm ($J_{Rh-P} = 175$ Hz) is in agreement with a chelating dppe ligand[13] in the heterotetranuclear framework, while the doublet centered at 32.8 ppm ($J_{Rh-P} = 158$ Hz) should correspond to a dppe ligand bridging the other two rhodium atoms.

Similarly, the reaction of **3** with 1 molar equiv of dppp gives the complex $[CpTi(\mu_3\text{-}S)_3Rh_3(CO)_4(\mu\text{-dppp})]$ (**14**). However, the reaction with a further molar equivalent of dppp leads to a mixture of species arising from the nonselective substitution of the carbonyl ligands. This mixture probably contains heterotetranuclear units linked by bridging dppp ligands, since the integrity of the heterotetranuclear framework is observed in the FAB mass spectrum. The IR spectrum of complex **14** (CH_2Cl_2) shows three strong absorptions that closely resemble those of complex **12**, and the chemical shift of the doublet in the $^{31}P\{^1H\}$ NMR spectrum is in agreement with a bridging coordination of the dppp ligand (Chart 2).

Compound **3** reacts with 1 equiv of the more rigid chiral diphosphine (*R*)-BINAP to give the complex $[CpTi(\mu_3\text{-}S)_3Rh_3(CO)_4(\eta^2\text{-}(R)\text{-BINAP})]$ (**15**), containing a chelating (*R*)-BINAP ligand. The $^{31}P\{^1H\}$ NMR spectrum of **15** shows inequivalent phosphorus nuclei, as expected from the asymmetry of the chiral ligand. The chelating coordination mode of the BINAP ligand is supported by both the observed chemical shift and the magnitude of the J_{P-P} coupling constant[14] and is probably a consequence of the stability of the seven-membered metallacycle formed. Complex **15** does not react with extra (*R*)-BINAP ligand at room temperature, although a nonselective replacement of the carbonyl ligands takes place at 323 K in toluene.

NMR Investigation of the Reaction of $[CpTi(\mu_3\text{-}S)_3\{Rh(CO)_2\}_3]$ with PPh_3. To gain insight into the observed selectivity of the substitution process with monodentate P-donor ligands, stepwise additions of PPh_3 to complex **3** and to the ^{13}CO-labeled complex $[CpTi(\mu_3\text{-}S)_3\{Rh(^{13}CO)_2\}_3]$ (**3***) have been carried out and monitored by IR and ^1H, $^{13}C\{^1H\}$, and $^{31}P\{^1H\}$ NMR spectroscopy. The replacement of the carbonyl groups of **3** by triphenylphosphine indicates that the conversion to $[CpTi(\mu_3\text{-}S)_3\{Rh(CO)(PPh_3)\}_3]$ (**5**) is neither stepwise nor simple. The process goes through three intermediate species (**4a**, **4b**, and **4c**; Chart 3) which maintain the heterotetranuclear framework.

Addition of 1 molar equiv of PPh_3 to **3*** in CD_2Cl_2 at 193 K gives a mixture which still contains the starting material **3*** (39%) and the intermediate species **4a*** (22%) and **4b*** (39%), as deduced from the integral of the Cp resonances in the ^1H NMR spectrum (at δ 6.08

(12) (a) Tunik, S. P.; Vlasov, A. V.; Gorshkov, N. I.; Starova, G. L.; Nikolskii, A. B.; Rybinskaya, M. I.; Batsanov, A. S.; Struchkov, Yu. T. *J. Organomet. Chem.* **1992**, *433*, 189. (b) Bordoni, S.; Heaton, B. T.; Seregni, C.; Strona, L.; Goodfellow, R. J.; Hursthouse, M. B.; Thornton-Pett, M.; Martinengo, S. *J. Chem. Soc., Dalton Trans.* **1988**, 2103.

(13) (a) Carmona, D.; Lamata, M. P.; Ferrer, J.; Modrego, J.; Perales, M.; Lahoz, F. J.; Atencio, R.; Oro, L. A. *J. Chem. Soc., Chem. Commun.* **1994**, 575. (b) Bruno, G.; De Munno, G.; Tresoldi, G.; Lo Schiavo, S.; Piraino, P. *Inorg. Chem.* **1992**, *31*, 1538.

(14) Pottier, Y.; Mortreux, A.; Petit, F. *J. Organomet. Chem.* **1989**, *370*, 333.

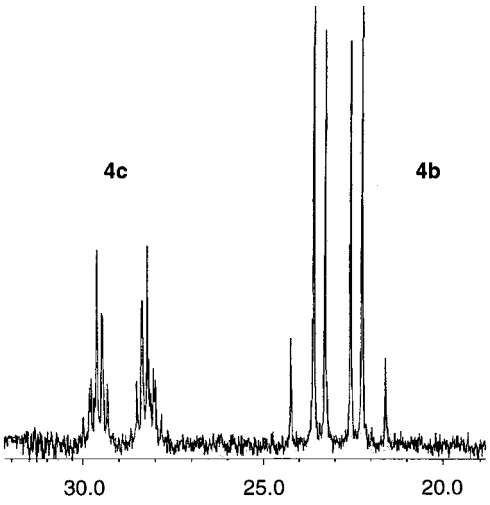

Figure 1. $^{31}P\{^1H\}$ NMR spectrum of $[CpTi(\mu_3\text{-}S)_3\{Rh(CO)(PPh_3)\}_3]$ (**5**) under an atmosphere of CO in $CDCl_3$ at 218 K, containing $[CpTi(\mu_3\text{-}S)_3Rh_3(\mu\text{-}CO)(CO)_4(PPh_3)_2]$ (**4b**) and $[CpTi(\mu_3\text{-}S)_3Rh_3(\mu\text{-}CO)(CO)_3(PPh_3)_3]$ (**4c**).

ppm, **3***; at 5.94 ppm, **4a***; at 5.01 ppm, **4b***). Increasing the amount of added PPh_3 results in the disappearance of **3*** in favor of the intermediate species **4b***. Thus, reaction of **3*** with 2.4 molar equiv of PPh_3 gives a mixture containing **4b*** (58%), **4c*** (33%, δ 5.31 ppm), and also a small amount of the final product **5*** (8%). The ^1H NMR spectrum after the addition of just 3 molar equiv of PPh_3 still shows the presence of **4c*** (88%) and **5*** (12%); however, fluxing out the carbon monoxide atmosphere with argon, in the NMR tube, results in the exclusive formation of the final compound $[CpTi(\mu_3\text{-}S)_3\{Rh(^{13}CO)(PPh_3)\}_3]$ (**5***).

Analysis of the spectroscopic information in CD_2Cl_2 at 193 K suggests that intermediate **4a** results from the substitution of one carbonyl ligand at one of the rhodium centers (Chart 3). Thus, $[CpTi(\mu_3\text{-}S)_3Rh_3(^{13}CO)_5(PPh_3)]$ (**4a***) shows a doublet of doublets at 32.8 ppm (J_{Rh-P} = 165.8 Hz, $^2J_{P-C}$ = 16.0 Hz) in the $^{31}P\{^1H\}$ NMR spectrum. In addition, the five carbonyl groups appear as five doublets of doublets in the $^{13}C\{^1H\}$ NMR spectrum. The resonance at 187.0 ppm (dd, J_{Rh-C} = 72.8 Hz, J_{P-C} = 16 Hz) corresponds to the carbonyl ligand of the "$Rh(^{13}CO)(PPh_3)$" unit and the resonances at 184.2 ppm (dd, J_{Rh-C} = 71.9 Hz, J_{C-C} = 6 Hz), 184.0 ppm (dd, J_{Rh-C} = 73.0 Hz, J_{C-C} = 6 Hz), 184.0 ppm (dd, J_{Rh-C} = 73.0 Hz, J_{C-C} = 6 Hz), and 183.0 ppm (dd, J_{Rh-C} = 70.0 Hz, J_{C-C} = 6 Hz) are due to the four carbonyl ligands of the two independent "$Rh(^{13}CO)_2$" units.

The intermediate **4b*** shows three strong ν(CO) absorptions for terminal carbonyls in the IR spectrum at 2056 (vs), 2016 (vs), and 1990 (s) cm^{-1} and a weak band at 1805 cm^{-1} corresponding to a bridging carbonyl ligand (μ_2-^{13}CO). The $^{31}P\{^1H\}$ NMR spectrum of unlabeled complex **4b** in $CDCl_3$ at 218 K (see Figure 1) displays an AA′XX′ spin system (A = ^{31}P and X = ^{103}Rh) at δ = 22.89 ppm, which shows the presence of two chemically equivalent triphenylphosphine ligands in the molecule. A successful simulation of the spectrum gives a standard $^1J_{Rh-P}$ coupling constant (165 Hz), a weak negative coupling $^2J_{Rh-P}$ (−0.90 Hz), and a strong $^3J_{P-P}$ coupling (117 Hz). The large value of the $^3J_{P-P}$ coupling constant suggests that both phosphorus atoms are coupled through a metal−metal bond and supports a transoid disposition of the subunit P−Rh−Rh−P in **4b**.

The $^{13}C\{^1H\}$ NMR spectrum of **4b*** (CD_2Cl_2, 193 K) (see Figure 2) has been properly simulated as the MM′N_2Q part of the spin system AA′MM′N_2QXX′ (A = ^{31}P, X = ^{103}Rh, M = N = Q = ^{13}C) (Figure 3). The bridging carbonyl ligand is observed as a virtual triplet of triplets at δ_Q = 223.72 ppm as a consequence of coupling to two pairs of chemically equivalent rhodium and phosphorus nuclei ($^1J_{Rh-C}$ = 40.0 Hz and $^2J_{P-C}$ = 14 Hz). A small coupling to the adjacent ^{13}CO ligands is also observed ($^2J_{C-C}$ = 3.0 Hz). These data indicate that the bridging carbonyl is placed between the two rhodium atoms bound to the triphenylphosphine ligands and are in agreement with the formulation of **4b** as $[CpTi(\mu_3\text{-}S)_3Rh_3(\mu\text{-}CO)(CO)_4(PPh_3)_2]$ having the C_s structure shown in Chart 3. The remaining four terminal carbonyl ligands in **4b*** are observed as two sets of chemically equivalent ligands in accordance with the proposed C_s symmetry. Thus, the carbonyl ligands of the subunit "$Rh(^{13}CO)_2$" display a doublet at δ_N 191.1 ppm ($^1J_{Rh-C}$ = 71.8 Hz) and the terminal carbonyl ligands in the subunit P−Rh−(μ-^{13}CO)−Rh−P are observed as a complex signal at δ 190.3 ppm resulting from coupling to Rh, P, and ^{13}C nuclei. A simulation of the signal shows standard $^1J_{Rh-C}$ (64.0 Hz) and $^2J_{P-C}$ (15.1 Hz) coupling constants and a small $^2J_{C-C}$ value (3.0 Hz).

The spectroscopic information and chemical behavior of **4c** are in agreement with the formulation $[CpTi(\mu_3\text{-}S)_3Rh_3(\mu\text{-}CO)(CO)_3(PPh_3)_3]$ (Chart 3). Thus, the intermediate **4c*** shows a strong absorption at 1976 cm^{-1} in the IR spectrum but also a weak band at 1799 cm^{-1}. However, the resonance of the bridging carbonyl ligand (μ_2-^{13}CO) is not detected in the $^{13}C\{^1H\}$ NMR spectrum in CD_2Cl_2 at 193 K, but a simple pseudoquartet centered at 200.2 ppm is observed for the four carbonyl ligands (see Figure 2). This suggests that all the carbonyl ligands undergo a rapid exchange at low temperature and became equivalent on the NMR time scale. This behavior is also found in the $^{31}P\{^1H\}$ NMR spectrum of **4c** in $CDCl_3$ at 218 K (see Figure 1), where a symmetric complex resonance is observed at 22.9 ppm. As the chemical exchange between the carbonyl ligands is not stopped at 193 K, the spin system to simulate the dynamic behavior of **4c** is not available. Nevertheless, a qualitative simulation of both ^{13}C and ^{31}P NMR spectra based on chemical intuition has been carried out.

The proposed frozen structure for **4c** derives from the replacement of one of the two carbonyl ligands of the "$Rh(CO)_2$" moiety in **4b** by a triphenylphosphine ligand. The stereochemistry of this rhodium center is open to debate. Although a square-planar coordination is expected to occur, a tetrahedral environment (Chart 3) is proposed on the basis of both the chemical behavior (vide infra) and the structure found for the related iridium complex $[CpTi(\mu_3\text{-}S)_3Ir_3(\mu\text{-}CO)(CO)_3\{(POMe)_3\}_3]$, which has recently been characterized.[10a] Since the scrambling of carbonyl ligands in cluster chemistry generally proceeds via a series of terminal-to-bridge carbonyl sequences,[15] the dynamic behavior could take place through a concerted movement of the carbonyl

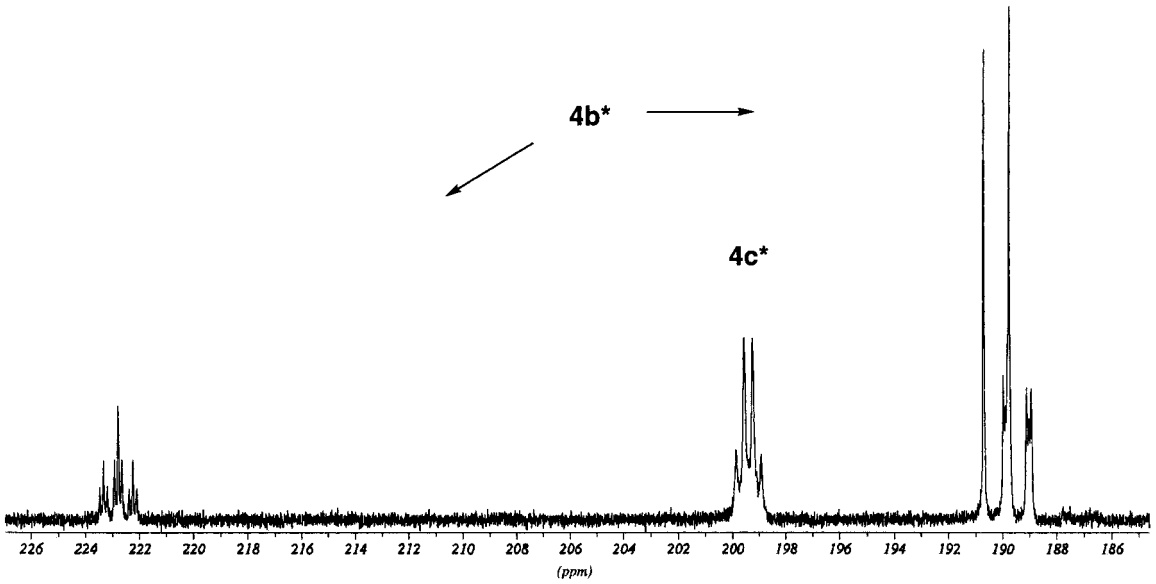

Figure 2. $^{13}C\{^1H\}$ NMR spectrum of [CpTi(μ_3-S)$_3${Rh(CO)(PPh$_3$)}$_3$] (**5**) (carbonyl region) under an atmosphere of ^{13}CO in CD_2Cl_2 at 193 K containing [CpTi(μ_3-S)$_3$Rh$_3$(μ-^{13}CO)(^{13}CO)$_4$(PPh$_3$)$_2$] (**4b***) and [CpTi(μ_3-S)$_3$Rh$_3$(μ-^{13}CO)(^{13}CO)$_3$(PPh$_3$)$_3$] (**4c***).

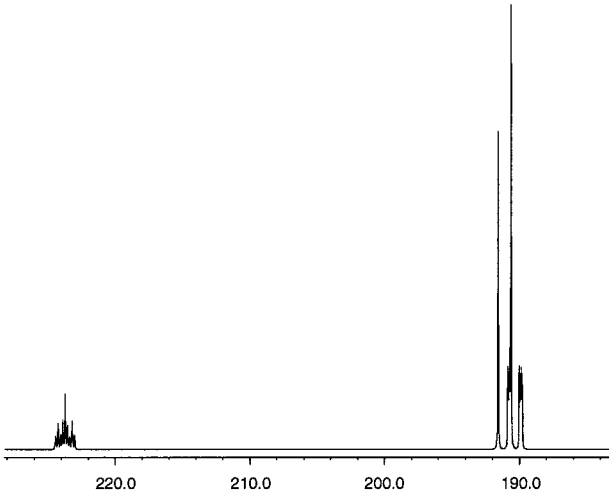

Figure 3. Simulated $^{13}C\{^1H\}$ NMR spectrum of [CpTi(μ_3-S)$_3$Rh$_3$(μ-^{13}CO)(^{13}CO)$_4$(PPh$_3$)$_2$] (**4b***) in the carbonyl region.

ligands underneath the triangle defined by the three rhodium atoms. A standard merry-go-round exchange process[16] involving the motion of the bridging μ_2-CO ligand to a terminal position at one rhodium center, accompanied by the conversion of its terminal carbonyl ligand to bridge the adjacent rhodium atom, is the proposed exchange mechanism (Figure 4). This process guarantees that after three individual exchanges all the carbonyls and triphenylphosphine ligands have visited each of the three sites in the structure.

A reliable simulation of the $^{31}P\{^1H\}$ NMR spectrum of **4c** at the fast exchange limit (Figure 5) has been achieved assuming a AA′XX′BY spin system (A = B = ^{31}P; X = Y = ^{103}Rh) and the exchange mechamism

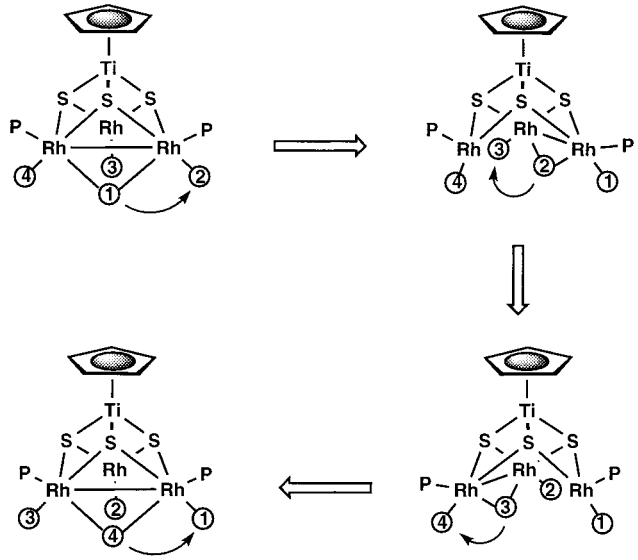

Figure 4. Carbonyl exchange mechanism proposed for the dynamic behavior of [CpTi(μ_3-S)$_3$Rh$_3$(μ-CO)(CO)$_3$(PPh$_3$)$_3$] (**4c**). Carbonyl ligands are represented by numbered circles; one of the triphenylphosphine ligands has been omitted for clarity.

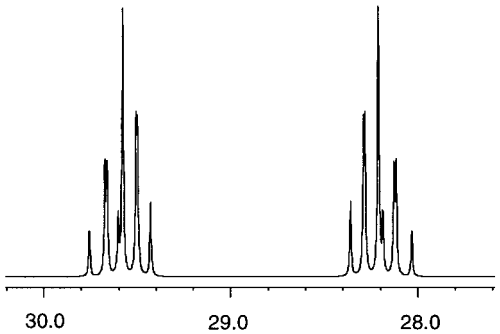

Figure 5. Simulated $^{31}P\{^1H\}$ NMR spectrum of [CpTi(μ_3-S)$_3$Rh$_3$(μ-CO)(CO)$_3$(PPh$_3$)$_3$] (**4c**).

described above ($k = 1.0e + 4\ s^{-1}$). The parameters used for this dynamic simulation ($\delta_A = \delta_{A'} = 28.889$ ppm and $\delta_B = 28.895$ ppm; $J_{A-X} = J_{A'-X'} = 165$ Hz, $J_{B-Y} = 170$

(15) (a) Fumagalli, A.; Bianchi, M.; Malatesta, M. C.; Ciani, G.; Moret, M.; Sironi, A. *Inorg. Chem.* **1998**, *37*, 1324. (b) Wang, D.; Shen, H.; Richmond, M. G.; Schwartz, M. *Organometallics* **1995**, *14*, 3636. (c) Aime, S.; Dastrú, W.; Gobetto, R.; Arce, A. J. *Organometallics* **1994**, *13*, 3737. (d) Robben, M. P.; Geiger, W. E.; Rheingold, A. L. *Inorg. Chem.* **1994**, *33*, 5615. (e) Casey, C. P.; Widenhoefer, R. A.; Hallenbeck, S. L.; Hayashi, R. K.; Gavney, J. A., Jr. *Organometallics* **1994**, *13*, 4720.

(16) (a) Cooke, J.; Takats, J. *Organometallics* **1995**, *14*, 698. (b) Riesen, A.; Frederick, F. W. B.; Ma, A. K.; Pomeroy, R. K.; Shipley, J. A. *Organometallics* **1991**, *10*, 3629.

Scheme 1

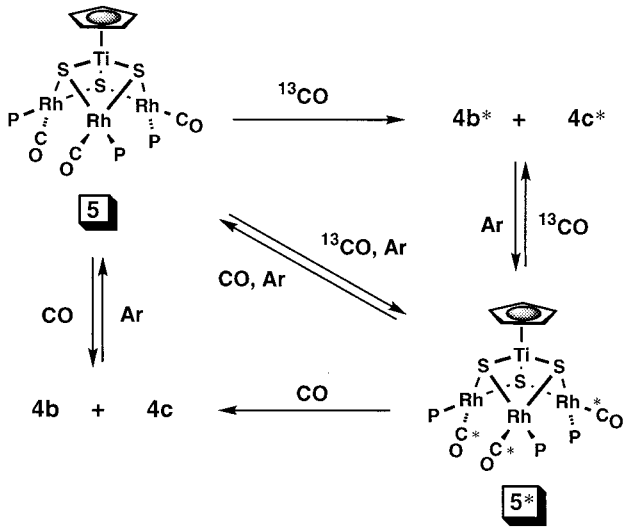

Hz, $J_{A-X'} = J_{A'-X} = -1.0$ Hz, and $J_{A-A'} = 60$ Hz) correlate well with those obtained from the calculated spectra for **4b** and are in good agreement with the proposed frozen structure.

The complex resonance observed at 200.2 ppm in the $^{13}C\{^1H\}$ NMR spectrum of **4c*** at the fast exchange limit is an average resonance resulting from the coalescence between the bridging (ca. 223 ppm) and terminal (ca. 191 ppm) carbonyl resonances as a consequence of the exchange process outlined above.

Reaction of [CpTi(μ_3-S)$_3${Rh(CO)(PPh$_3$)}$_3$] (5) with Carbon Monoxide. As expected from the stepwise synthesis of [CpTi(μ_3-S)$_3${Rh(CO)(PPh$_3$)}$_3$] (**5**), this complex reacts with carbon monoxide at atmospheric pressure in dichloromethane to give a black solution which contains the complexes [CpTi(μ_3-S)$_3$Rh$_3$(μ-CO)(CO)$_4$(PPh$_3$)$_2$] (**4b**; 85%), [CpTi(μ_3-S)$_3$Rh$_3$(μ-CO)(CO)$_3$(PPh$_3$)$_3$] (**4c**; 15%), and free PPh$_3$, as observed by $^{31}P\{^1H\}$ NMR spectroscopy at low temperature (Figure 1). However, replacement of the carbon monoxide atmosphere by argon gives quantitatively the starting complex **5**. Analogously, complex **5** reacts with ^{13}CO to rapidly give the labeled complexes **4b*** and **4c***, as detected by $^{13}C\{^1H\}$ NMR (Figure 2). This mixture can be converted to **5*** by purging the ^{13}CO from the solution with argon.

Interestingly, complex **5** can be transformed into **5***, through the intermediates **4b*** and **4c***, by reaction with ^{13}CO, and consequently, the reaction of **5*** with CO gives **5** through the intermediates **4b** and **4c** (Scheme 1).

CpTi(μ_3-S)$_3${Rh(cod)}$_3$] (1) and [CpTi(μ_3-S)$_3$-{Rh(tfbb)}$_3$] (2) as Catalyst Precursors in the Hydroformylation of Olefins. The heterotetranuclear complexes [CpTi(μ_3-S)$_3${Rh(diolef)}$_3$] (diolef = tfbb (**1**), cod (**2**)), in the presence of phosphorus ligands, have been used as catalytic precursors in the hydroformylation of hex-1-ene and styrene under mild conditions of temperature and pressure. As has been shown in the reactivity studies, both complexes give identical species in the presence of carbon monoxide and the added phosphorus ligand. Thus, the effect of different phosphorus ligands in the hydroformylation reaction has been studied. It is noteworthy that no hydrogenation or isomerization products are observed in any case.

Hydroformylation of Hex-1-ene. When **1** or **2** is used as the catalytic precursor in the presence of PPh$_3$ (P/Rh ratio = 2, 4) in the hydroformylation of hex-1-ene, at 5 bar and 353 K (entries 1 and 2, Table 1), a 96% conversion to aldehydes is obtained together with a 77% regioselectivity for the linear aldehyde.

Table 1. Hydroformylation of 1-Hexene[a]

run no.	precursor	L	P/Rh	*t* (h)	% conversn[b]	% *n*
1	**1**	PPh$_3$	2	8	96	77
2	**1**	PPh$_3$	4	8	96	78
3	**2**	PPh$_3$	6	24	45	85
4[c]	**2**	TPPMS	2	24	58	78
5	**2**	P(OMe)$_3$	2	24	34	82
6	**2**	dppe	2	24	9	76
7	**2**	dppe	4	24	74	50

[a] Reaction conditions: 5 bar, 353 K, 1-hexene (10 mmol), catalyst precursor (0.05 mmol), toluene (7.5 mL), CO/H$_2$ = 1. [b] Aldehyde conversion measured by GC. [c] Solvent methanol.

A higher P/Rh ratio provides a better selectivity for the linear aldehyde (85%), although lower conversion is obtained (entry 3, Table 1). It is generally accepted that several different species may coexist under hydroformylation conditions. In this particular case, the change in the selectivity observed at high P/Rh ratios indicates that the active species should be different and suggests that a species which contains more phosphorus ligands coordinated to the metal could be present. Taking into account the equilibrium observed between the different heterotetranuclear species containing carbonyl and phoshine ligands (Scheme 1), and in order to know which of those intermediates is formed under CO pressure, we have carried out a high-pressure NMR spectroscopic study.

A solution of complex **2** in the presence of PPh$_3$ (P/Rh = 2) in toluene-d_8 at room temperature under a nitrogen atmosphere was studied after being pressurized to 2.5 bar of carbon monoxide. In the $^{31}P\{^1H\}$ NMR spectrum recorded at 213 K, an equilibrium between the species [CpTi(μ_3-S)$_3$Rh$_3$(μ-CO)(CO)$_4$(PPh$_3$)$_2$] (**4b**) and [CpTi(μ_3-S)$_3$Rh$_3$(μ-CO)(CO)$_3$(PPh$_3$)$_3$] (**4c**) is observed. The same experiment, but with an increase in the P/Rh ratio to 6, shows that the species **4c**, in which each rhodium center contains a phosphorus ligand, becomes predominant. Thus, the variation of the active species could be the reason for the higher selectivity and lower conversion observed using this P/Rh ratio in the hydroformylation reaction.

On the other hand, the $^{31}P\{^1H\}$ NMR and IR spectra of the solutions obtained at the end of the hydroformylation experiments both show, with a P/Rh ratio of 2, 4, or 6, the presence of the heterotetranuclear species **5**, indicating that the heterotetranuclear framework is maintained under hydroformylation conditions.

Taking into account the increasing interest in water-soluble catalysts, the monosulfonated triphenylphosphine TPPMS was also utilized as the phosphorus ligand. This system is active in hydroformylation in methanol maintaining the regioselectivity observed for the triphenylphosphine system, but a lower activity is found (entry 4, Table 1). On the other hand, when trimethyl phosphite is used as the phosphorus ligand, a lower conversion to aldehydes with a higher regioselectivity for the linear aldehyde is obtained (entry 5, Table 1).

The hydroformylation of hex-1-ene has also been carried out in the presence of the diphosphine dppe.

Table 2. Hydroformylation of Styrene Using [CpTi(μ_3-S)$_3${Rh(tfbb)}$_3$] (2)[a]

run no.	*P* (bar)	L	P/Rh	% conversn[b]	% 2-PP[c]	% ee
1	10	PPh_3	2	70	88	
2	30	PPh_3	4	88	89	
3[d]	10	$P(OPh)_3$	2	90	75	
4	10	dppe	2	25	81	
5	10	dppe	4	42	75	
6	10	dppp	2	36	92	
7	10	(−)-CHP	2	32	96	<1[f]
8	10	(−)-CHP	4	51	95	<1[f]
9	10	(−)-BDPP	2	95	94	5 (*R*)[f]
10	10	(−)-BDPP	4	99	95	5 (*R*)[f]
11	10	(+)-BINAP	2/3	18	91	15 (*S*)[e]
12	10	(+)-BINAP	2	48	91	9 (*S*)[e]

[a] Reaction conditions: 353 K, t = 24 h, styrene (10 mmol), complex (0.05 mmol), tetrahydrofuran (7.5 mL), CO/H_2 = 1. [b] Aldehyde conversion measured by GC. [c] 2-Phenylpropanal. [d] t = 5 h. [e] % ee was measured by chiral GC on the 2-phenylpropanol obtained by reduction of the aldehydes with $LiAlH_4$. [f] % ee was measured by chiral GC on the 2-phenylpropanoic acid obtained by oxidizing the aldehydes with $KMnO_4$.

With a P/Rh ratio of 2 a low conversion to aldehydes (entry 6, Table 1) is observed. However, when the P/Rh ratio is raised to 4, a 74% conversion to aldehydes is obtained, although no selectivity is observed (entry 7, Table 1). Similar trends in activity and selectivity have been previously observed by Hughes et al.[17]

Precursors **1** and **2**, in the presence of phosphite ligands such as $P(OPh)_3$ and $P(o\text{-}OC_6H_4{}^tBu)_3$, which are more π-acidic than PPh_3 or $P(OMe)_3$, give systems that are inactive for the hydroformylation of hex-1-ene under the same conditions. More basic phosphines such as PCy_3 and PMe_3 do not show catalytic activity either. If we take into account the large cone angle differences between the pairs, PCy_3 (θ = 170°) and PMe_3 (θ = 118°), and $P(o\text{-}OC_6H_4{}^tBu)_3$ (θ = 175°) and $P(OPh)_3$ (θ = 128°), the lack of catalytic activity should be attributed to electronic rather than steric effects.

Hydroformylation of Styrene. The complex [CpTi(μ_3-S)$_3${Rh(tfbb)}$_3$] (**2**) in the presence of PPh_3 does not shown any catalytic activity at 5 bar and 353 K. However, a 70% conversion to aldehydes is obtained at 10 bar at the same temperature, although the rate of conversion of styrene is lower than in the case of the hydroformylation of hex-1-ene (entry 1, Table 2). Increasing the pressure to 30 bar and the P/Rh ratio to 4 gives 87% conversion, and the regioselectivity is maintained (entry 2, Table 2).

As was observed in the hydroformylation of hex-1-ene, the ^{31}P NMR spectrum of the solutions and IR spectra recorded after hydroformylation of styrene are characteristic of the tetranuclear structure [CpTi(μ_3-S)$_3$Rh$_3$(CO)$_3$(PR$_3$)$_3$] (**5**).

The use of the phosphite $P(OPh)_3$ as ligand increases the activity in the hydroformylation of styrene and a 90% conversion is obtained in 5 h together with a 75% regioselectivity for 2-phenylpropanal. This effect is opposite to the one observed in the hydroformylation of hex-1-ene (entry 3, Table 1) using triphenyl phosphite as P-donor ligand.

It is well-known that, normally, monodentate phosphines are poor inducers in the asymmetric hydroformylation of styrene.[18] Thus, to explore the effect of the added phosphorus ligand and the possibilities of this system for the asymmetric hydroformylation of styrene, the diphosphines dppe and dppp have been studied.[19] Complex **2** in the presence of dppe at 10 bar and 353 K gave 25% conversion to aldehydes with 81% regioselectivity for 2-phenylpropanal (entry 4, Table 2). A higher P/Rh ratio also leads to a higher conversion to aldehydes, although a lower regioselectivity is observed. At the same pressure and temperature but using dppp as phosphorus ligand, 92% regioselectivity is obtained (entry 6, Table 2).

Chiral diphosphines have been also extensively used as ligands in Rh and Pt catalyst precursors for enantioselective hydroformylation.[20,21] In this context, we have studied the potential of complex **2** in the asymmetric hydroformylation of styrene. Hydroformylation in the presence of the chiral diphosphines (−)-CHP ((2*S*,3*S*)-bis(diphenylphosphino)butane), (−)-BDPP ((2*S*,4*S*)-(−)-2,4-bis(diphenylphosphino)pentane), and (−)-BINAP ((*S*)-(−)-2,2′-bis(diphenylphosphino)-1,1′-binaphthyl) gave regioselectivities higher than 90%; however, the highest enantiomeric excess observed is 15% (entries 7−12, Table 2). It has been reported that the use of BDPP as a chiral ligand in different rhodium systems provides considerable enantiomeric excesses (up to 56%). However, an excess of diphosphine ligand is required to obtain asymmetric induction.[22] A recent study of the intermediates under hydroformylation conditions has led to the characterization of the predominant species in this Rh/BDPP system as mononuclear.[23] The heterotetranuclear system shows only low enantiomeric excesses, independent of the P/Rh ratio used under the same conditions, suggesting the presence of different catalytic species (entries 9 and 10, Table 2).

Discussion

Replacement reactions with P-donor ligands in the complex [CpTi(μ_3-S)$_3${Rh(CO)$_2$}$_3$] (**3**) are highly selective. Thus, the C_3 isomer of [CpTi(μ_3-S)$_3${Rh(CO)(PR$_3$)}$_3$] (**5**−**10**) is the only product formed in the case of monodentate phosphine and phosphite ligands. In contrast, the same replacement reactions with monodentate phosphine or phosphite ligands in the iridium heterotetranuclear complex [CpTi(μ_3-S)$_3${Ir(CO)$_2$}$_3$] give rise to the clusters [CpTi(μ_3-S)$_3$Ir$_3$(μ-CO)(CO)$_3$(PR$_3$)$_3$], which incorporate a bridging carbonyl ligand.[10a]

The study of the reaction of [CpTi(μ_3-S)$_3${Rh(CO)$_2$}$_3$] (**3**) with PPh_3 allows us to gain insight into the equilibria leading to the selective replacement of the carbonyl groups toward the C_3 isomer. Monitoring of the reaction at room temperature showed a fluxional behavior of the involved intermediates, but successful

(17) Hughes, O. R.; Unruh, J. D. *J. Mol. Catal.* **1981**, 12, 71−83.

(18) (a) Ogata, I.; Ikeda, Y.; Asakawa, T. *Kogyo Kagaku Zasshi* **1971**, *74*, 1839. (b) Laï, R.; Ucciani, E. *J. Mol. Catal.* **1978**, *4*, 401. (c) Brown, C. K.; Wilkinson, G. *J. Chem. Soc. A* **1970**, 2753.

(19) (a) Beller, M.; Cornils, B.; Frohning, C. D.; Kholpainter, C. W. *J. Mol. Catal. A* **1995**, *104*, 17. (b) Gladiali, S.; Bayon, J. C.; Claver, C. *Tetrahedron: Asymmetry* **1995**, *6*, 1453.

(20) Gladiali, S.; Bayón, J. C.; Claver, C. *Tetrahedron: Asymmetry* **1995**, *6*, 1453.

(21) Agbossou, F.; Carpentier J. F.; Mortreux, A. *Chem. Rev.* **1995**, *95*, 2485.

(22) Masdeu-Bultó, A. M.; Orejón, A.; Castellanos, A.; Castillón, S.; Claver C. *Tetrahedron: Asymmetry* **1996**, *7*, 1829.

(23) Castellanos, A.; Castillón, S.; Claver, C.; van Leeuwen, P. W. N. M.; Lange, W. G. J. *Organometallics* **1998**, *17*, 2543.

Scheme 2

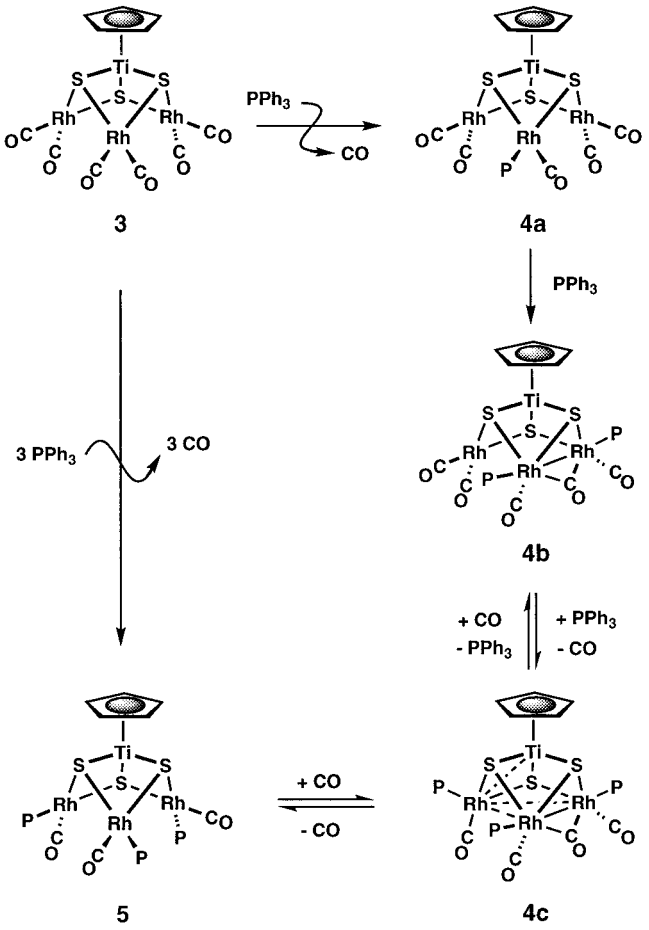

characterization by multinuclear NMR spectroscopy is only possible at low temperature. The structure of the three intermediate species (**4a**, **4b**, and **4c**) and the chemical behavior of the complex $[CpTi(\mu_3\text{-}S)_3\{Rh(CO)(PPh_3)\}_3]$ (**5**) under carbon monoxide suggest the mechanism outlined in Scheme 2 for the formation of **5** starting from **3**. The first intermediate, $[CpTi(\mu_3\text{-}S)_3Rh_3(CO)_5(PPh_3)]$ (**4a**), results from the expected replacement of one carbonyl ligand by PPh_3 at a single d^8 rhodium center in **3**. However, the incorporation of a second equivalent of PPh_3 is not followed by carbonyl elimination and results in the formation of $[CpTi(\mu_3\text{-}S)_3Rh_3(\mu\text{-}CO)(CO)_4(PPh_3)_2]$ (**4b**), which contains a bridging carbonyl ligand between two rhodium atoms. Replacement of one of the carbonyl ligands in **4b** leads to $[CpTi(\mu_3\text{-}S)_3Rh_3(\mu\text{-}CO)(CO)_3(PPh_3)_3]$ (**4c**), which gives **5** by decarbonylation.

It is noticeable that an iridium complex with a formula identical with that of **4b** is also involved in the transformation of $[CpTi(\mu_3\text{-}S)_3\{Ir(CO)_2\}_3]$ to $[CpTi(\mu_3\text{-}S)_3Ir_3(\mu\text{-}CO)(CO)_3(PR_3)_3]$;[10a] however, the intermediate containing only one PPh_3 ligand is different from **4a**, since the introduction of the first PPh_3 ligand is not followed by the carbonylation and, therefore, the cluster $[CpTi(\mu_3\text{-}S)_3Ir_3(\mu\text{-}CO)(CO)_5(PR_3)_3]$ is formed first. This observation could be interpreted in terms of the higher ability of iridium to form metal−metal bonds.[24]

Complexes **4b** and **4c** are 62-electron clusters which most probably contain a single Rh−Rh bond and a bridging carbonyl ligand. However, although both species are fluxional at room temperature, their behavior is quite different, since **4c** is still dynamic down to 193 K. The proposed structures for both species differ only in the coordination and stereochemistry of the rhodium atom not engaged in the metal−metal bond. Thus, the square-planar coordination in **4b** is evidenced by the $MM'N_2Q$ spin system observed in the carbonyl region of the $^{13}C\{^1H\}$ NMR spectrum. However, despite this fact, the dynamic $^{31}P\{^1H\}$ NMR spectrum of **4c** has been qualitatively simulated assuming a static AA′XX′BY spin system and a tetrahedral rhodium (C_s symmetry). The spectrum can also be calculated with an ABCXYZ spin system and square-planar rhodium atom (C_1 symmetry) with the same exchange mechanism as proposed in Figure 3 and similar chemical shifts ($\delta_A \approx \delta_B \approx \delta_C$). The tetrahedral stereochemistry at the rhodium center proposed in **4c** results in an overall C_s symmetry and relies on the solid-state structure found for the related iridium complex $[CpTi(\mu_3\text{-}S)_3Ir_3(\mu\text{-}CO)(CO)_3\{(POMe)_3\}_3]$,[10a] which also exhibits a carbonyl scrambling comparable to that observed in **4c**.

It is worth mentioning that the equilibria **4b** ⇌ **4c** ⇌ **5** and the dynamic behavior of complex **4c** are likely to be the factors responsible for the complete and rapid replacement between ^{13}CO and CO ligands which permit the conversion between **5** and **5***. This interpretation is in agreement with the lack of evident carbonyl scrambling in **4b** under the same conditions, probably due to the stereochemistry of the third rhodium center, which hinders the motion of the carbonyl ligands, and to the presence of a localized metal−metal bond. However, the replacement of one of the carbonyl ligands in **4b** by PPh_3 provides the stereochemical change necessary to allow the carbonyl exchange and also involves the concerted migration of the metal−metal bond in a parallel fashion to the bridging carbonyl.[25]

Once the structure of the intermediates **4a**, **4b**, and **4c** and their transformations indicated in Scheme 2 have been determined, the observed stereoselectivity in the formation of the complexes of the type $[CpTi(\mu_3\text{-}S)_3\{Rh(CO)(PR_3)\}_3]$ (**5**−**11**) should be a consequence of the decarbonylation of **4c**. Thus, a concerted stereochemical rearrangement of the three "$Rh(CO)(PR_3)$" fragments should take place after the removal of one of the carbonyl ligands to produce the C_3 isomer exclusively. This should be a facile process, since complex **5** smoothly incorporates an extra carbonyl ligand to give **4c**, which easily undergoes the replacement of one of the triphenylphosphine ligands by carbon monoxide to give **4b**.

The equilibrium **4b** ⇌ **4c** ⇌ **5** is also relevant to the catalytic activity shown by the catalyst precursors $[CpTi(\mu_3\text{-}S)_3\{Rh(diolef)\}_3]$ (diolef = tfbb (**1**), cod (**2**)) in the hydroformylation of hex-1-ene and styrene under mild conditions of pressure and temperature. In fact, the species **4b** and **4c** are observed by HPNMR spectroscopy at low temperature under hydroformylation conditions (2.5 bar of CO and 2.5 bar of H_2). Unfortunately, spectroscopic information in the presence of substrate at higher temperature is not accessible due to fluxionality.

(24) Tejel, C.; Bordonada, M.; Ciriano, M. A.; Edwards, A. J.; Clegg, W.; Lahoz, F. J.; Oro, L. A. *Inorg. Chem.* **1999**, *38*, 1108.

(25) (a) Houser, E. J.; Venturelli, A.; Rauchfuss, T. B.; Wilson, S. R. *Inorg. Chem.* 1**995**, *34*, 6402. (b) Venturelli, A.; Rauchfuss, T. B. *J. Am. Chem. Soc.* **1994**, *116*, 4824. (c) Houser, E. J.; Amarasekera, J.; Rauchfuss, T. B.; Wilson, S. R. *J. Am. Chem. Soc.* **1991**, *113*, 7440.

As far as the catalytic activity is concerned, the results presented in Tables 1 and 2 show that electronic factors are dominant over steric ones in the case of monodentate P-donor ligands. The reported results seems to indicate that tetranuclear species could be present during the hydroformylation process.

Conclusions

The chemical behavior of the early−late heterobimetallic complexes $[CpTi(\mu_3\text{-}S)_3\{RhL_2\}_3]$ shows the stability of the heterotetranuclear framework in both stoichiometric and catalytic reactions. In particular, the metal framework in $[CpTi(\mu_3\text{-}S)_3\{Rh(CO)_2\}_3]$ is maintained in replacement reactions with phosphine, phosphite, and diphosphine P-donor ligands. The synthesis of the complexes $[CpTi(\mu_3\text{-}S)_3\{Rh(CO)(PR_3)\}_3]$ is selective toward the more symmetrical isomer. The complex $[CpTi(\mu_3\text{-}S)_3\{Rh(CO)(PPh_3)\}_3]$ (**5**) reacts reversibly with carbon monoxide to give the 62-electron clusters **4b** and **4c**, which are in equilibrium. Interestingly, both species are intermediates in the formation of **5**. Multinuclear NMR spectroscopic characterization of the intermediates leading to the synthesis of the trisubstituted complex **5** suggest that the decarbonylation of **4c** is the key step for the observed stereoselectivity. Finally, HPNMR spectroscopic studies have shown that the clusters **4b** and **4c** are formed under hydroformylation conditions using the diolefinic precursor $[CpTi(\mu_3\text{-}S)_3\{Rh(diolef)\}_3]$ (diolef = tfbb (**1**), cod (**2**)) and triphenylphosphine.

Experimental Section

General Considerations. All manipulations were performed under an inert atmosphere (nitrogen or argon) using Schlenk-tube techniques. Solvents were dried by standard methods and distilled under nitrogen immediately prior to use.

Physical Measurements. ^{1}H, ^{13}C{^{1}H}, and ^{31}P{^{1}H} NMR spectra were recorded on Varian UNITY, Bruker ARX 300, and Varian Gemini 300 spectrometers operating at 299.95, 75.47, and 121.49 MHz, 300.13, 75.47, and 121.49 MHz, and 300.08, 75.46, and 121.47 MHz, respectively. Chemical shifts are reported in ppm and referenced to Me_4Si using the signal of the deuterated solvent (^{1}H and ^{13}C) and 85% H_3PO_4 (^{31}P) as external references, respectively. Assignments in complex NMR spectra were done by simulation with the program gNMR (version 3.6; Cherwell Scientific Publishing Ltd) for Macintosh. The initial choice of chemical shifts and coupling constants was optimized by succesive iterations following a standard least-squares procedure; a numerical assignment of the experimental frequencies was used. IR spectra were recorded on a Nicolet IR 550 spectrometer (4000−400 cm^{-1}) as Nujol mulls between polyethylene sheets or in solution in a cell with NaCl windows. Elemental analyses were performed with a Perkin-Elmer 2400 microanalyzer. Mass spectra were recorded in a VG Autospec double-focusing mass spectrometer operating in the FAB$^+$ mode. Ions were produced with the standard Cs$^+$ gun at ca. 30 kV; 3-nitrobenzyl alcohol (NBA) was used as matrix. Gas chromatography analyses were performed on a Hewlett-Packard Model 5890, a gas chromatograph with a flame ionization detector using a 25 m × 0.2 mm i.d. capillary column (Ultra 2). Enantiomeric excesses were measured on the same equipment using a 50 m × 0.25 mm i.d. capillary column after reduction or oxidation of the aldehydes[22] (FS-cyclodex β-I/P).

Catalysis. Low-pressure hydroformylation experiments were carried out in a specially designed autoclave with magnetic stirring. The catalytic solution was contained in a glass vessel. Constant temperature was maintained by circulating water through a double jacket. The gas mixture was introduced at constant pressure from a gas ballast. The drop in pressure in the ballast was monitored using a pressure transducer connected to an electronic measurement and printing unit. High-pressure hydroformylation experiments (30 atm) were carried out in a Berghof autoclave, and the reaction mixtures were magnetically stirred and electrically heated.

Standard Catalysis Experiment. A solution of the substrate (10 mmol), the catalyst precursor (0.05 mmol), and the phosphorus compound in 7.5 mL of solvent were charged into the evacuated autoclave. The gas mixture was introduced, and the system was heated. When the thermal equilibrium was reached, the gas mixture was introduced until the desired pressure was obtained and stirring was initiated. After the reaction time, the autoclave was cooled to room temperature and depressurized. The samples were analyzed by gas chromatography.

HPNMR Experiments. The in situ HPNMR experiments were carried out in a sapphire tube (i.d. = 10 mm). The heterotetranuclear complex $[CpTi(\mu_3\text{-}S)_3\{Rh(cod)\}_3]$ (15 mg, 0.018 mmol) and PPh_3 (28.4 mg, 0.11 mmol or 85 mg, 0.32 mmol) were dissolved in toluene-d_8 (1.5 mL) under a nitrogen atmosphere, and the sapphire tube was closed. After the mixture was pressurized with CO or CO/H_2, the NMR spectra were recorded immediately.

Synthesis of the Complexes. The complexes $[CpTi(\mu_3\text{-}S)_3\{Rh(diolef)\}_3]$ (diolef = tfbb (**1**), cod (**2**)), $[CpTi(\mu_3\text{-}S)_3\{Rh(CO)_2\}_3]$ (**3**), and $[CpTi(\mu_3\text{-}S)_3\{Rh(CO)(PPh_3)\}_3]$ (**5**) were prepared as previously described.[10a]

$[CpTi(\mu_3\text{-}S)_3\{Rh(^{13}CO)_2\}_3]$ (3*). An orange suspension of $[CpTi(\mu_3\text{-}S)_3\{Rh(cod)\}_3]$ (**2**; 0.150 g, 0.178 mmol) in hexane (5 mL) was stirred under carbon-13 monoxide (^{13}CO, 99%) to give a red suspension in 30 min. The red solid was isolated by filtration, washed with cold hexane, and dried under vacuum. Yield: 0.096 g (79%). MS (FAB$^+$, CH_2Cl_2, *m/z*): 692 (M$^+$, 75%), 663 (M$^+$ − ^{13}CO, 100%). ^{1}H NMR (CD_2Cl_2, 298 K, δ): 6.08 (s, Cp). ^{13}C{^{1}H} NMR (CD_2Cl_2, 298 K, δ): 183.1 (d, J_{Rh-C} = 72 Hz, CO). IR (CH_2Cl_2, cm^{-1}): ν(CO), 2043 (s), 2008 (m), 1983 (s).

$[CpTi(\mu_3\text{-}S)_3\{Rh(^{13}CO)(PPh_3)\}_3]$ (5*). A solution of PPh_3 (0.118 g, 0.450 mmol) in dichloromethane (5 mL) was added to a solution of the complex $[CpTi(\mu_3\text{-}S)_3\{Rh(^{13}CO)_2\}_3]$ (**3***; 0.104 g, 0.150 mmol) in dichloromethane (10 mL) to give a yellow solution after evolution of carbon monoxide. The mixture was stirred for 30 min and then concentrated under vacuum to ca. 1 mL. Slow addition of hexane gave an orange microcrystalline solid which was isolated by filtration, washed with cold hexane, and dried under vacuum. Yield: 0.164 g (79%). MS (FAB$^+$, CH_2Cl_2, *m/z*): 1391 (M$^+$, 30%), 1332 (M$^+$ − 2^{13}CO, 35%), 1303 (M$^+$ − 3^{13}CO, 40%), 1099 (M$^+$ − ^{13}CO − PPh_3, 100%). ^{1}H NMR (CD_2Cl_2, 298 K, δ): 7.63 (m, 18H, PPh_3), 7.34 (m, 27H, PPh_3), 5.74 (s, 5H, Cp). ^{31}P{^{1}H} NMR ($CDCl_3$, 298 K, δ): 35.5 (dd, J_{Rh-P} = 166 Hz, J_{P-C} = 16 Hz). ^{13}C{^{1}H} NMR (CD_2Cl_2, 298 K, δ): 188.3 (dd, J_{Rh-C} = 74 Hz, J_{C-P} = 16 Hz, CO). IR (CH_2Cl_2, cm^{-1}): ν(CO), 1935 (s).

$[CpTi(\mu_3\text{-}S)_3\{Rh(CO)(PR_3)\}_3]$ (6−10). The addition of a solution of the corresponding tertiary phosphine PR_3, or phosphite $P(OR)_3$ (0.210 mmol), in dichloromethane (5 mL) to a solution of $[CpTi(\mu_3\text{-}S)_3\{Rh(CO)_2\}_3]$ (**3**; 0.048 g, 0.070 mmol) in dichloromethane (10 mL) gave yellow-orange solutions after evolution of carbon monoxide. The solutions were stirred for 30 min and then concentrated under vacuum to ca. 1 mL. Slow addition of *n*-hexane gave the compounds as yellow microcrystalline solids which were isolated by filtration, washed with cold hexane, and then vacuum-dried.

$[CpTi(\mu_3\text{-}S)_3\{Rh(CO)(PMe_3)\}_3]$ (6). Yield: 86%. Anal. Calcd for $C_{17}H_{32}O_3P_3Rh_3S_3Ti$: C, 24.59; H, 3.88. Found: C, 24.54; H, 3.76. MS (FAB$^+$, CH_2Cl_2, *m/z*): 830 (M$^+$, 28%), 801 (M$^+$ − CO, 55%), 773 (M$^+$ − 2CO, 40%), 745 (M$^+$ − 3CO, 100%).

^{1}H NMR ($CDCl_3$, 298 K, δ): 5.86 (s, 5H, Cp), 1.68 (d, 27H, J_{P-H} = 9.0 Hz, PMe_3). $^{31}P\{^1H\}$ NMR ($CDCl_3$, 298 K, δ): −6.4 (d, J_{Rh-P} = 156 Hz). IR (CH_2Cl_2, cm^{-1}): ν(CO), 1962 (s).

[CpTi(μ_3-S)$_3${Rh(CO)(PCy$_3$)}$_3$] (7). Yield: 80%. Anal. Calcd for $C_{62}H_{104}O_3P_3Rh_3S_3Ti$: C, 51.59; H, 7.26. Found: C, 51.53; H, 7.33. MS (FAB$^+$, CH_2Cl_2, *m*/*z*): 1444 (M^+, 50%), 1416 (M^+ − CO, 25%), 1388 (M^+ − 2CO, 12%), 1358 (M^+ − 3CO, 45%). ^{1}H NMR ($CDCl_3$, 298 K, δ): 5.69 (s, 5H, Cp), 1.21−2.50 (m, 99H, PCy_3). $^{31}P\{^1H\}$ NMR ($CDCl_3$, 298 K, δ): 48.7 (d, J_{Rh-P} = 162 Hz). IR (CH_2Cl_2, cm^{-1}): ν(CO), 1946 (s).

[CpTi(μ_3-S)$_3${Rh(CO)(P(OPh)$_3$)}$_3$] (8). Yield: 63%. Anal. Calcd for $C_{62}H_{50}O_{12}P_3Rh_3S_3Ti$: C, 48.58; H, 3.29. Found: C, 48.53; H, 3.11. MS (FAB$^+$, CH_2Cl_2, *m*/*z*): 1532 (M^+, 7%), 1504 (M^+ − CO, 7%), 1476 (M^+ − 2CO, 7%), 1194 (M^+ − CO − $P(OPh)_3$, 53%), 1166 (M^+ − 2CO − $P(OPh)_3$, 47%), 1138 (M^+ − 3CO − $P(OPh)_3$, 75%). ^{1}H NMR ($CDCl_3$, 298 K, δ): 7.06−7.24 (m, 45H, $P(OPh)_3$), 5.28 (s, 5H, Cp). $^{31}P\{^1H\}$ NMR ($CDCl_3$, 298 K, δ): 138.5 (d, J_{Rh-P} = 284 Hz). IR (CH_2Cl_2, cm^{-1}): ν(CO), 2008 (s).

[CpTi(μ_3-S)$_3${Rh(CO)(P(OMe)$_3$)}$_3$] (9). Yield: 91%. Anal. Calcd for $C_{17}H_{32}O_{12}P_3Rh_3S_3Ti$: C, 20.96; H, 3.31. Found: C, 20.76; H, 2.09. MS (FAB$^+$, CH_2Cl_2, *m*/*z*): 975 (M^+, 15%), 946 (M^+ − CO, 45%), 918 (M^+ − 2CO, 73%), 890 (M^+ − 3CO, 100%). ^{1}H NMR ($CDCl_3$, 298 K, δ): 5.81 (s, 5H, Cp), 3.64 (d, 27H, J_{P-H} = 12.6 Hz, $P(OMe)_3$). $^{31}P\{^1H\}$ NMR ($CDCl_3$, 298 K, δ): 137.1 (d, J_{Rh-P} = 261 Hz). IR (CH_2Cl_2, cm^{-1}): ν(CO), 1996 (s).

[CpTi(μ_3-S)$_3${Rh(CO)(P(OC$_6$H$_4$^{t}Bu)$_3$}$_3$] (10). Yield: 63%. Anal. Calcd for $C_{98}H_{122}O_{12}P_3Rh_3S_3Ti$: C, 57.76; H, 6.03. Found: C, 57.74; H, 5.55. MS (FAB$^+$, CH_2Cl_2, *m*/*z*): 1530 (M^+ − CO − $P(OC_6H_4{}^tBu)_3$, 60%), 1501 (M^+ − 2CO − $P(OC_6H_4$-^{t}Bu)$_3$, 25%). ^{1}H NMR ($CDCl_3$, 298 K, δ): 7.67 (d, 9H, J_{H-H} = 8.01 Hz), 7.25 (d, 9H, J_{H-H} = 7.78 Hz), 6.89 (t, 9H, J_{H-H} = 7.09 Hz), 6.77 (t, 9H, J_{H-H} = 6.90 Hz) ($P(OC_6H_4{}^tBu)_3$), 4.86 (s, 5H, Cp), 1.32 (s, 81H, ^{t}Bu). $^{31}P\{^1H\}$ NMR ($CDCl_3$, 298 K, δ): 114.6 (d, J_{Rh-P} = 285 Hz). IR: (CH_2Cl_2, cm^{-1}): ν(CO), 2012 (s).

[CpTi(μ_3-S)$_3${Rh(CO)(TPPMS)}$_3$] (11). Solid TPPMS·$2H_2O$ (0.065 g, 0.162 mmol) was added to a solution of [CpTi(μ_3-S)$_3${Rh(CO)(PPh_3)}$_3$] (**5**; 0.075 g, 0.054 mmol) in THF (6 mL) to give an orange suspension in 5 min. The suspension was stirred for 30 min and filtered to give an orange solid, which was washed with THF and vacuum-dried. Yield: 0.065 g (71%). ^{1}H NMR (CD_3OD, 293 K, δ): 8.01−7.24 (m, 42H, TPPMS), 5.69 (s, 5H, Cp). $^{31}P\{^1H\}$ NMR (MeOD, 293K, δ): 36.8 (d, J_{Rh-P} = 169 Hz). IR: (Nujol, cm^{-1}): ν(CO), 1983 (s).

[CpTi(μ_3-S)$_3$Rh$_3$(CO)$_4$(μ-dppe)] (12). dppe (0.029 g, 0.073 mmol) was added to a solution of [CpTi(μ_3-S)$_3${Rh(CO)$_2$}$_3$] (**3**; 0.050 g, 0.073 mmol) in dichloromethane (5 mL) to give a yellow solution after evolution of carbon monoxide. The solution was stirred for 15 min and then concentrated under vacuum. Slow addition of *n*-hexane gave the complex as a pale orange microcrystalline solid which was filtered, washed with *n*-hexane, and vacuum-dried. Yield: 0.058 g (77%). Anal. Calcd for $C_{35}H_{29}O_4P_2Rh_3S_3Ti$: C, 40.88; H, 2.84. Found. C, 40.78; H, 2.80. MS (FAB$^+$, CH_2Cl_2, *m*/*z*): 1028 (M^+, 9%), 1000 (M^+ − CO, 6%), 971 (M^+ − 2CO, 25%), 943 (M^+ − 3CO, 28%), 915 (M^+ − 4CO, 47%). ^{1}H NMR ($CDCl_3$, 298 K, δ): 7.30−7.65 (m, 20H, PPh_2), 5.93 (s, 5H, Cp), 3.15 (m, 2H, CH_2, dppe), 2.60 (m, 2H, CH_2, dppe). $^{31}P\{^1H\}$ NMR ($CDCl_3$, 298 K, δ): 30.7 (d, J_{Rh-P} = 163 Hz). IR: (CH_2Cl_2, cm^{-1}): ν(CO), 2060 (vs), 2006 (vs), 1979 (s).

[CpTi(μ_3-S)$_3$Rh$_3$(μ-dppe)(CO)$_2$(η^2-dppe)] (13) was obtained as a brown-orange solid by reaction of [CpTi(μ_3-S)$_3${Rh(CO)$_2$}$_3$] (**3**; 0.050 g, 0.073 mmol) with dppe (0.058 g, 0.146 mmol) in dichloromethane following the procedure described above. Yield: 0.070 g (75%). Anal. Calcd. for $C_{59}H_{53}O_2P_4Rh_3S_3Ti$: C, 51.70; H, 3.90. Found: C, 51.45; H, 3.75. MS (FAB$^+$, CH_2Cl_2, *m*/*z*): 970 (M^+ − dppe, 15%), 942 (M^+ − dppe − CO, 55%), 914 (M^+ − dppe − 2CO, 100%). ^{1}H NMR ($CDCl_3$, 298 K, δ): 7.20−7.76 (m, 40H, PPh_2), 5.68 (s, 5H, Cp), 3.13 (m, 2H, CH_2 dppe), 2.49 (m, 2H, CH_2, dppe), 2.19 (m, 4H, CH_2, dppe). $^{31}P\{^1H\}$ NMR ($CDCl_3$, 298 K, δ): 65.5 (d, J_{Rh-P} = 175 Hz), 32.8 (d, J_{Rh-P} = 158 Hz). IR (CH_2Cl_2, cm^{-1}): ν(CO), 1971.

[CpTi(μ_3-S)$_3$Rh$_3$(CO)$_4$(μ-dppp)] (14) was obtained as an orange microcrystalline solid by reaction of [CpTi(μ_3-S)$_3${Rh(CO)$_2$}$_3$] (**3**; 0.050 g, 0.073 mmol) with dppp (0.030 g, 0.073 mmol) in dichloromethane following the procedure described above. Yield: 0.061 g (80%). Anal. Calcd for $C_{36}H_{31}O_4P_2Rh_3S_3Ti$: C, 41.48; H, 3.00. Found: C, 41.37; H, 2.87. MS (FAB$^+$, CH_2Cl_2, *m*/*z*): 1043 (M^+, 23%), 1015 (M^+ − CO, 32%), 986 (M^+ − 2CO, 100%). ^{1}H NMR ($CDCl_3$, 298 K, δ): 7.30−7.52 (m, 20H, PPh_2), 5.87 (s, 5H, Cp), 2.87 (m, 2H, CH_2, dppp), 2.45 (m, 4H, CH_2, dppp). $^{31}P\{^1H\}$ NMR ($CDCl_3$, 298 K, δ): 36.1 (d, J_{Rh-P} = 169 Hz). IR (CH_2Cl_2, cm^{-1}): ν(CO), 2060 (vs), 2006 (vs), 1981 (s).

[CpTi(μ_3-S)$_3$Rh$_3$(CO)$_4$(η^2-(*R*)-BINAP)] (15) was obtained as a brown-orange solid by reaction of [CpTi(μ_3-S)$_3${Rh(CO)$_2$}$_3$] (**3**; 0.052 g, 0.076 mmol) with (*R*)-BINAP (0.047 g, 0.076 mmol) in dichloromethane following the procedure described above. Yield: 0.080 g (84%). Anal. Calcd for $C_{53}H_{37}O_4P_2Rh_3S_3Ti$: C, 50.82; H, 2.98. Found: C, 50.73; H, 2.73. MS (FAB$^+$, CH_2Cl_2, *m*/*z*): 1252 (M^+, 40%), 1225 (M^+ − CO, 15%), 1197 (M^+ − 2CO, 53%), 1168 (M^+ − 3CO, 12%), 1140 (M^+ − 4CO, 22%). ^{1}H NMR ($CDCl_3$, 298 K, δ): 7.32−7.49 (m), 7.22 (m), 6.94 (t), 6.86 (t), 6.69 (m), 6.48 (d), 6.40 (d) (BINAP), 5.58 (s, 5H, Cp). $^{31}P\{^1H\}$ NMR ($CDCl_3$, 298 K, δ): 42.0 (dd, J_{Rh-P} = 176 Hz, J_{P-P} = 47 Hz), 33.2 (dd, J_{Rh-P} = 171 Hz, J_{PP} = 47 Hz). IR: (CH_2Cl_2, cm^{-1}): ν(CO), 2064 (vs), 2050 (vs), 2004 (vs).

Acknowledgment. Financial support from the Dirección General de Enseñanza Superior (DGES, Projects PB97-407-C05-1, PB95-221-C02-1, and PB94-1186), the CYTED Homogeneous Catalysis Network, and a fellowship from the Diputación General de Aragón (M.A.C.) is gratefully acknowledged.

OM990155J